



## Effects of various ion solutions on phosphorus adsorption in the sediments of a water body that originated from agricultural land subsidence and submergence caused by coal mining activities

Kai Xie<sup>a,b</sup>, Yanqiu Zhang<sup>a</sup>, Qitao Yi<sup>c,\*</sup>, Jiaping Yan<sup>c</sup>

<sup>a</sup>*School of Environment Science and Spatial Informatics, China University of Mining and Technology, Xuzhou 221116, China*

<sup>b</sup>*School of Sciences, Anhui University of Science and Technology, Huainan 232001, China*

<sup>c</sup>*School of Earth and Environmental Science, Anhui University of Science and Technology, Huainan 232001 China*

Tel. +86-152-1554-6045; email: qtyi@aust.edu.cn

Received 29 September 2012; Accepted 11 November 2012

---

### ABSTRACT

Extensive subsidence and submergence of agricultural land has been caused by coal mining activities in the Huainan Coal Mine Area, China. Considering the site-specific regional water chemistry, we investigated the influence of ion solutions on phosphorus (P) adsorption behavior in the sediments of a 20-year-old body of water. The P isothermal adsorption was measured in four different types of ion solutions, prepared through additions of sodium chloride (NaCl), calcium chloride (CaCl<sub>2</sub>), sodium bicarbonate (NaHCO<sub>3</sub>), a mixture of sodium bicarbonate and calcium chloride (NaHCO<sub>3</sub> + CaCl<sub>2</sub>), and ultra pure water (deionized water with specific resistivity reaching the value of 18 MΩ cm) as a control. The sediments parameters analyzed included P-fractions, organic matter (OM), iron oxides, clay, and others, with the aim of analyzing their individual effects on P adsorption. Cationic calcium (Ca<sup>2+</sup>) was to found to enhance P adsorption ability, while a weakly alkaline environment (simulated through NaHCO<sub>3</sub> addition) reduced it. The effects of ion solutions on P adsorption potential were in the order CaCl<sub>2</sub> > NaHCO<sub>3</sub> + CaCl<sub>2</sub> > NaCl > ultra pure water > NaHCO<sub>3</sub>. The two-dimensional structure of lake sediments overlying inundated agricultural soil could be responsible for the observed differences between sediment properties and P adsorption features in different layers of sediments.

*Keywords:* Coal mine; Sediments; Land subsidence; Phosphorus; Isothermal adsorption

---

### 1. Introduction

Extensive land subsidence has been caused by coal mining activities in China. In plains with locally high groundwater levels, these subsided pockets of land can be seasonally or permanently flooded. As a result, it generally lends itself to the formation of unique

types of water bodies, which can be classified as collapsed ponds, reservoirs, or lakes, according to their shapes and scales. These types of water bodies are widely distributed in the coal mining areas of the Huang-Huai-Hai Plain in China. For instance, it has led to the formation of a subsidence area of 150 km<sup>2</sup>, with one-third of it covered by water in the Xuzhou Coal Mine Area, Jiangsu Province. The subsided land

---

\*Corresponding author.

area is more than 250 km<sup>2</sup> in the Huainan and Huaibei Coal Mine Area, Anhui Province, with 100 km<sup>2</sup> being submerged permanently [1]. In addition, these areas of subsidence display a trend of expansion, increasing in area by 3–5% per year due to continuous mining activities.

Due to the subsidence and flooding of agricultural land, traditional agricultural ecosystems have been completely transformed into freshwater systems in the forms of collapsed ponds, reservoirs, or lakes. The sedimentary environment of this water area originated from agricultural soil, which is typically rich in nutrients due to long histories of fertilization and cultivation activities. The potential for nutrient release from the soil to the overlying water is one of the important and interesting issues for the site-specific research into such ecosystems. Of particular importance is phosphorus (P) internal loading and its contribution to the eutrophication status of lakes, rivers, or estuaries, which have been widely researched [2–4]. Even if small amounts of P migrate from the cultivation layer to the overlying water column, it would result in a significant increase in water P concentration, and furthermore, impact the overall nutrient status of the freshwater system.

Submerged soils undergo more reductive conditions, with an apparently higher P release potential from the P-pool of the cultivation layer. The primary mechanisms for P migration are generally considered to be coupled with the reduction of Fe (III) hydroxides. As Fe (II) production occurs, phosphate anions chemically associated with Fe (III) oxides are desorbed and released [5,6]. The transfer of appreciable P-pools to soil or sediment solutions could play an important role in P bioavailability in many ecosystems such as wetlands, reservoirs, inundated forests, or cultivation soils undergoing cyclical dry and wet conditions [7–9].

After the submergence of agricultural land in the studied area, the original unsaturated zone of the soils became saturated with water, and the relationship between groundwater and surface water became active through the sediment interface. Accordingly, the ion movement caused by water exchange may have an important influence on P transport and on other trace elements as well, particularly on those that are generally involved in active surface behaviors, e.g. adsorption, ion exchange, sedimentation, etc. However, there are a few studies of the effects of ion solutions on P mobility at the interface of the solid phase (sediment) and its ambient solution. The bicarbonates of the local water are high with a slightly alkaline pH [10]. Major cationic ions include Na<sup>+</sup>, Ca<sup>2+</sup>, and Mg<sup>2+</sup>. On the one hand, alkaline conditions are likely to desorb P bound with metal hydroxides [11]. On the

other hand, Ca<sup>2+</sup> can enhance the effect of P immobilization on the surface of the soils or sediments. Phosphate could be adsorbed and partitioned on calcite surfaces or precipitated with calcium ions [12]. For instance, in lake restoration practices, Ca(OH)<sub>2</sub> treatment led to lower P flux in sediments [13]. CaCO<sub>3</sub> was also found to be effective in decreasing the soluble P content of pore water in wetland soil [14].

The impact of sediments on dissolved forms of P can be assessed by performing sorption experiments. A variety of protocols exist for conducting such experiments, and the specific methods used can greatly influence results [15]. Generally, the Langmuir and the Freundlich equations are the most widely used in environmental applications to characterize sorption parameters (e.g. P sorption maxima, kinetic equilibrium constant, and equilibrium P concentration) [16]. However, for low concentrations, the P adsorption equation was typically linear, allowing these characterized parameters to be obtained via linear regression [17]. There are three characterized parameters in the linear-fit equation, the zero equilibrium P concentrations (EPC<sub>0</sub>), the slope of the fit curve (*k* constant), and the *y*-axis intercept (*b*). The EPC<sub>0</sub> (mg/L) is a measure of the P concentration at which sediment is neither adsorbing nor desorbing P. When the dissolved P concentration of ambient sediments is bigger than EPC<sub>0</sub>, net adsorption occurs. When it is smaller than EPC<sub>0</sub>, desorption occurs. *k* (L/kg) constant reflects the bonding energy at sorption affinity. *b* value (mg/kg) is the native adsorbed phosphorous (NAP) that had been adsorbed on the sediment prior to the experiments.

When concerning P behaviors, such as adsorption or release, past studies placed greater emphasis on controlling factors, such as pH or redox potentials, but few discussions were related to the actual effects of the ambient ion solution on P adsorption. Therefore, there are two objectives in this paper: (1) to discuss the potential for P migration in sediments based on their properties and the chemical P-fraction in the specific research site and (2) to determine the effect of ion solutions on P adsorption behavior, in order to uncover the crucial factors ultimately determining P mobility or immobilization.

## 2. Materials and methods

### 2.1. Site description

The Panxie Coal Mine Area is located on the flood plain of the Huai River Watershed, which is one of the seven biggest watersheds in China. It covers an area of 865 km<sup>2</sup> with a maximum width of 6 km and a maximum length of 25 km. Due to about 50 years of

continuous and intensive resource exploitation, a pocket of subsided land with an area of 150 km<sup>2</sup> has formed, of which, two-thirds is submerged. The water body selected for research is located in the eastern part of the Panyi Coal Mine and has a surface area of approximately 4 km<sup>2</sup> (Fig. 1). Twenty years ago, before subsidence and submergence, it existed as cropland. The local soil genus is classified as the *yellow fluvo-aquic soil*, a common soil species in the flooding plain. It is used primarily for aquaculture, without fish feed addition, by local farmers. This water body is connected with the Ni River, which receives effluent from coal mine drainage, pollutants from rural non-point sources, and domestic sewage from surrounding villages. If the annual deposition rate of sediments is estimated to be 1–4 mm, based on analogies of lake sedimentation, the original cultivation layer is probably covered by significant sediment layers of 2–8 cm.

2.2. Water sampling and analysis

Annual investigations into water quality parameters were conducted in the spring (May) and summer (August) 2011. Surface water samples were taken, and

water parameters, including pH, dissolved oxygen (DO), Secchi disc transparency (T), chemical oxygen demand (COD), total nitrogen (TN), total phosphorus (TP), soluble reactive phosphate (SRP), chlorophyll-*a* (Chl-*a*), and constant ions (bicarbonate, chloride, sulfate, sodium, magnesium, and calcium), were examined, according to a previously published method [18,19]. Means of the water parameters in nine sampling sites (Fig. 1) and their viabilities in the investigated water bodies are summarized in Table 1. Water chemistry parameters for local shallow ground waters and coal mine effluents were obtained from a local geological survey report [10].

The average depth of the studied water body is 3.0 m, resembling a shallow lake. It is rich in DO with a weakly alkaline pH caused by local water chemistry. It also receives drainage water from deep coal mines, which is of high salinity (containing NaCl), and exhibits a fairly complex array of dissolved ions (Table 1). The water quality exhibits a eutrophic status with relatively low transparency, high nutrient content, and high Chl-*a* content according to the trophic state index for lakes proposed by Carson [20].

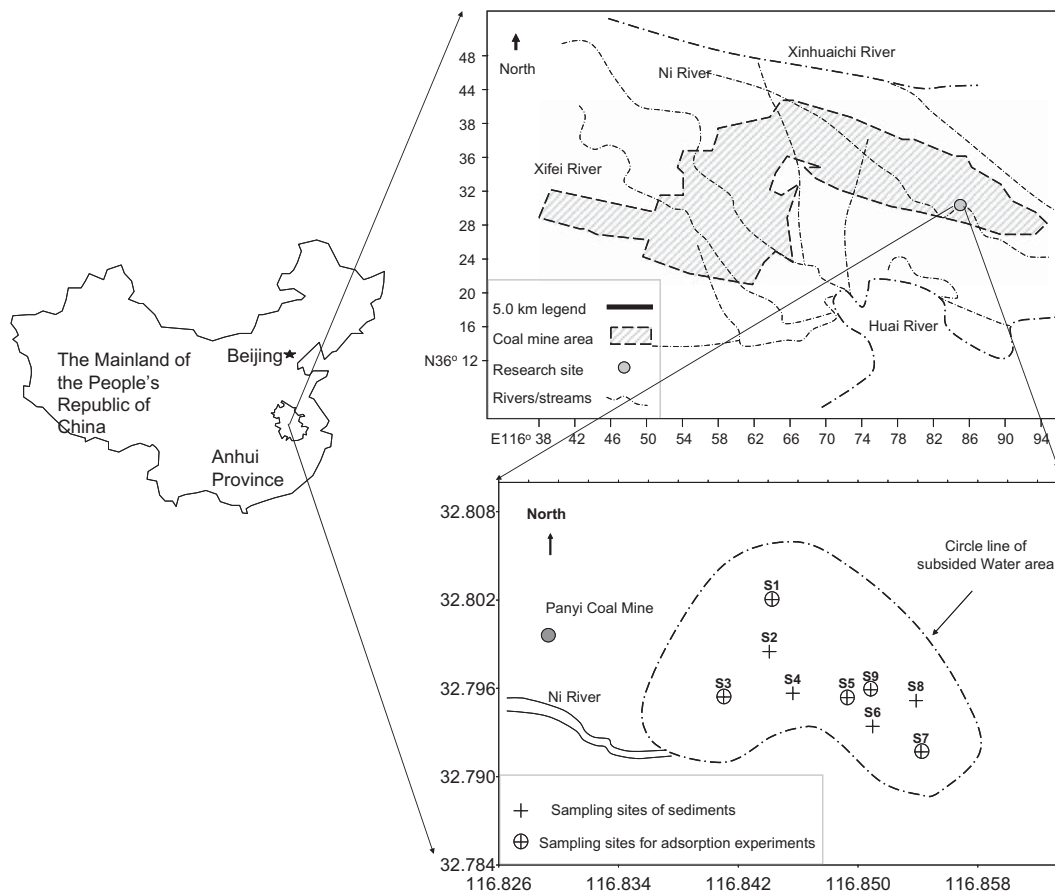


Fig. 1. Location of the Panxie Coal Mine Area and sampling sites of the subsided water body at the Panyi Coal Mine.

Table 1  
Characteristics of the studied water body and local water chemistry

Researched water body <sup>a</sup>	Major ions (meq/L)	HCO <sub>3</sub> <sup>-</sup>	Cl <sup>-</sup>	SO <sub>4</sub> <sup>2-</sup>	Na <sup>+</sup>	K <sup>+</sup>	Ca <sup>2+</sup>	Mg <sup>2+</sup>	Chl-a (µg/L)
	Nutrients status (mg/L)	pH	DO	T <sup>c</sup> (m)	COD <sub>cr</sub>	TN	TP	SRP	
		8.9±0.2	12.3±1.3	0.80±0.1	32.8±5.8	2.0±0.44	0.14±0.44	0.003±0.002	32.0±5.1
Local shallow ground water <sup>b</sup>	Major ions (meq/L)	HCO <sub>3</sub> <sup>-</sup>	Cl <sup>-</sup>	SO <sub>4</sub> <sup>2-</sup>	Na <sup>+</sup>	K <sup>+</sup>	Ca <sup>2+</sup>	Mg <sup>2+</sup>	
		6.60±0.69	0.66±0.22	0.27±0.07	2.76±0.95	0.12±0.00	2.28±0.41	2.44±0.72	
Discharge of coal mine <sup>b</sup>		7.13±0.92	21.48±5.37	3.40±0.82	28.60±4.79	0.20±0.01	1.51±0.75	1.64±0.41	

<sup>a</sup>Mean of values observed in 2011 during the spring and summer of nine sampling sites.

<sup>b</sup>Data from local geological survey.

<sup>c</sup>Secchi disc transparency.

### 2.3. Sediment sampling and analysis

Sediment sampling in the studied area was conducted in April 2011 using a corer sampler. Undisturbed sediment/interface cores were extruded and extended down through the entire cultivation layer (around 20 cm deep). Cores were obtained in nine different sites (marked as "S1–S9" sampling sites in Fig. 1). Sediments cores collected from the sample sites were averagely sliced into five thick layers from top to bottom after overlying water was partially drained. These sub-samples of each sediments core were labeled as "Layer 1, Layer 2, Layer 3, Layer 4, and Layer 5" from the top to the bottom, in order to assist with the description of the vertical profile of different parameters of sediments. A total of 45 sub-samples of sediments were sealed in plastic bags, kept cool in the field, and after being transported to the laboratory, they were air-dried at room temperature, homogenized, and size-fractionated to less than 100 µm using stainless steel sieves. The sediment samples were analyzed for pH, size fraction, organic matter (OM), P-fractions, TN, TP, Fe and Mn hydroxides, and cation exchange capacities (CEC).

Particle size distributions were determined by the traditional method of wet-sieving and sedimentation, as performed for general soil texture assessment, since the main part of the obtained sediments were composed of submerged agricultural soils. This method also ensured consistency of results with those of the local soils survey which was used in the study. Particulates less than 63 µm fraction was distinguished as silts and clays of the sediments after the removal of OM with hydrogen peroxide and dispersion with sodium metaphosphate. The OM represents the oxidizable matter remaining after the treatment of the sample with chromic acid/H<sub>2</sub>SO<sub>4</sub> according to the Walkey–Black method [21,22]. Concentrations of TP, iron, and manganese were determined after wet digestion with HCl, HNO<sub>3</sub>, HF, and HClO<sub>4</sub> sequentially [21]. The CEC was determined after extraction with 1 M CH<sub>3</sub>COONH<sub>4</sub> [21,22]. Iron and manganese in amorphous or poorly crystalline constituents were extracted using acidic ammonium oxalate (respectively, named as Fe<sub>o</sub> and Mn<sub>o</sub>). Iron and manganese in crystalline forms were extracted from dithionite–citrate–bicarbonate (namely, Fe<sub>d</sub>). Extracted Fe and Mn were measured by flame atomic absorption spectroscopy (FAAS).

The method of sequential extraction, which was proposed by Psenner et al. [23] with slight modifications by Hupfer et al. [24], was used to determine the P-fractionation of sediments. Sub-samples were subjected to sequential chemical extraction with 1 M

$\text{NH}_4\text{Cl}$ , 0.11 M  $\text{NaHCO}_3 + \text{Na}_2\text{S}_2\text{O}_4$ , 1 M  $\text{NaOH}$ , and 0.5 M  $\text{HCl}$ . The extracts were centrifuged and the supernatants were filtered through a 0.45  $\mu\text{m}$  cellulose acetate membrane. The SRP in each fraction was determined by the molybdenum blue/ascorbic acid method [18]. This extraction procedure fractionates sedimentary P into loosely sorbed P ( $\text{NH}_4\text{Cl-P}$ ), reductant soluble phosphorus (BD-P), metal oxide bound phosphorus ( $\text{NaOH-P}$ ), and calcium bound phosphorus ( $\text{HCl-P}$ ). Organic P was determined by calculating the difference between TP and inorganic phosphorus (IP), which was determined by extracting sediments with 1.0 M  $\text{H}_2\text{SO}_4$  before and after combustion at 500°C for two hours.

#### 2.4. P isothermal adsorption experiments

Sediment samples from sites S1, S3, S5, S7, and S9 were selected for P isothermal adsorption experiments. Sub-samples in layers 1, 3, and 5 from the above sites were analyzed to represent the surface, middle, and bottom layers of sediments, respectively. A sample of 0.25 g of sediment was mixed with a 25 mL solution of eight different initial P concentrations in a 50 mL polypropylene centrifuge tube. The P-solutions were prepared in four types of different solutions, namely,  $\text{NaCl}$ ,  $\text{CaCl}_2$ ,  $\text{NaHCO}_3$ , and  $\text{NaHCO}_3 + \text{CaCl}_2$  using the pure water (deionized water with specific resistivity of 18 M $\Omega$ cm) as a control (Table 2). The  $\text{NaHCO}_3 + \text{CaCl}_2$  solution group was assumed to reflect a local actual ion solution while other groups were measured to investigate the individual effects of ion solutions of  $\text{Na}^+$ ,  $\text{Ca}^{2+}$ , and  $\text{HCO}_3^-$  (weakly alkaline) on P adsorption behavior on the surfaces of sediments. In each group, solutions with initial P concentrations were prepared as follows: 0.00, 0.01, 0.02, 0.04, 0.08, 0.10, 0.16, and 0.20 mg/L (P content was adjusted using  $\text{KH}_2\text{PO}_4$ ).

For P isothermal adsorption experiments, the tubes were shaken at  $25 \pm 1^\circ\text{C}$  for 24 h. The suspensions were then centrifuged (2000 g  $\times$  30 min) and the supernatants were filtered through 0.45  $\mu\text{m}$  cellulose acetate membranes. The pH values of the equilibrated

solutions were recorded. The P concentrations in the solutions were determined spectrophotometrically using the molybdenum blue method. The adsorbed P was then calculated based on the difference between the initial amount of P added and the amount in the equilibrium solution. All of the above analyses were conducted in duplicate with the data presented as arithmetic means. In all, 600 data-sets were obtained from five groups multiplied by eight discrete P concentrations and 15 sub-samples of three layers of cores from five sites. Therefore, the statistical analysis was robust and is assumed to be reasonably accurate.

As discussed in the introduction, we used the program SPSS12.0 for mathematical descriptions of sorption isotherms, by fitting data-sets with linear functions:  $Q = kC_e + b$ , where  $Q$  is the P sorption amount (mg/kg).  $k$  (slope) is the sorption constant (L/kg), reflecting the bonding energy at sorption affinity.  $b$  (inset, mg/kg) is the NAP.

The  $\text{EPC}_0$  was determined graphically as the  $x$ -intercept of the plot of the zero amount of P absorbed at the  $y$ -axis against the  $C_e$  concentrations at the  $x$ -axis. Correlation analyses of sediment properties and adsorption parameters were performed by calculating Pearson correlation coefficients at a confidence level of 95 ( $p < 0.05$ ) and 99% ( $p < 0.01$ ) to investigate significant differences within different parameters.

### 3. Results and discussion

#### 3.1. Sediment properties and P-fraction characteristics

The statistical summaries of P-fractions and the selected parameters of sediments are summarized in Table 3 and 4. Furthermore, the profiles of P-fractions along core depths are indicated in Fig. 2. Almost all the P-fractions displayed an increasing trend from the bottom layers to the surface layers.

The mean TP concentration was 204.9 mg/kg across the bottom layer of sediments, and averaged 343.7 mg/kg in the sediments of surface layers. The IP ranged from 163.9 to 257.2 mg/kg, accounting for 73.3–81.5% of TP. The OP ranged from 16.2 to

Table 2  
Ion solution groups for P isothermal adsorption experiments

Group settings	Concentration (meq/L)	Equilibrium pH	Solution characteristics
Pure water group	–	6.9	Control
$\text{NaCl}$ group	4.0	7.1	Cationic sodium
$\text{CaCl}_2$ group	4.0	7.0	$\text{Ca}^{2+}$
$\text{NaHCO}_3$ group	4.0	7.8	Cationic sodium in weakly alkaline environment
$\text{NaHCO}_3 + \text{CaCl}_2$ group	4.0 + 4.0	7.7	Representing actual ion solution in the lake

Table 3  
Summary statistics of P-fractions in different layers in the studied area (unit: mg/kg)

Layer	NH <sub>4</sub> Cl-P		BD-P		NaOH-P		HCl-P		IP		OP		TP	
	Ave.	Std.	Ave.	Std.	Ave.	Std.	Ave.	Std.	Ave.	Std.	Ave.	Std.	Ave.	Std.
1	0.95	0.79	66.4	10.6	100.1	17.9	95.9	22.3	257.2	27.7	86.4	25.7	343.7	39.9
2	0.87	0.34	48.9	7.8	91.1	23.7	83.1	23.9	220.5	22.8	61.5	13.8	282.0	26.0
3	0.71	0.33	36.3	6.7	82.9	27.5	74.0	23.0	185.5	27.4	59.2	14.6	244.7	23.9
4	0.40	0.35	24.7	10.9	87.0	42.6	64.3	27.4	176.4	44.3	40.0	15.6	216.4	37.8
5	0.33	0.22	16.2	13.7	85.0	49.2	63.6	29.8	163.9	61.0	40.9	16.5	204.9	48.9

Table 4  
Summary statistics for OM, Fe (as Fe<sub>2</sub>O<sub>3</sub>), and Mn oxide (Mn<sub>o</sub>) contents in different layers of sediments

Layer	OM (%)		Total Fe (%)		Fe <sub>d</sub> (%)		Fe <sub>o</sub> (%)		Mn (%)		Mn <sub>d</sub> (%)		Mn <sub>o</sub> (%)	
	Mean	Std. dev.	Mean	Std. dev.	Mean	Std. dev.	Mean	Std. dev.	Mean	Std. dev.	Mean	Std. dev.	Mean	Std. dev.
1	2.04	1.14	6.10	1.08	1.13	0.16	0.65	0.13	0.078	0.022	0.039	0.007	0.045	0.009
2	1.24	0.83	5.18	0.79	1.11	0.20	0.58	0.11	0.076	0.016	0.033	0.006	0.039	0.007
3	0.82	0.27	4.92	0.60	1.10	0.19	0.58	0.12	0.065	0.016	0.032	0.006	0.042	0.007
4	0.69	0.18	4.81	0.41	1.12	0.19	0.52	0.07	0.056	0.012	0.032	0.008	0.044	0.012
5	0.80	0.38	4.37	0.41	1.14	0.23	0.38	0.10	0.053	0.013	0.034	0.010	0.043	0.014

66.4 mg/kg, accounting for 18.5–24.7% of TP. For IP species, the ranked order was NaOH-P > HCl-P > BD-P > NH<sub>4</sub>Cl-P, and their respective values were in the range of 85.0–100.1 mg/kg (28.6–41.3% of total IP), 63.6–95.9 mg/kg (27.4–30.9%), 16.2–66.4 mg/kg (7.9–19.9%), and less than 1 mg/kg, from the bottom to top layers, respectively.

Overall, TP was measured to be at moderate levels compared to the values reported in other studies on lakes [2]. However, BD-P and NaOH-P content was higher than HCl-P, which usually typifies the environmental conditions in eutrophic lakes [4,25]. The NaOH-P represents P bound to metal oxides, mainly Al and Fe, which can be again desorbing in basic solutions. Measurement of NaOH-P can be used for the estimation of both short-term and long-term available P in sediments. This fraction could be released, increasing the likelihood of phytoplankton blooms, which are accompanied by an increase in pH values [3] or an increase in anoxia at the sediment–water interface [26].

The contents of OM, Fe, and Mn oxides are listed in Table 4. Mean OM content ranged from 0.69 to 2.04% from the bottom to surface layers, displaying the same trends as TP. Total Fe concentration ranged from 4.37 to 6.10%. Mean dithionite-extractable iron (Fe<sub>d</sub>) was 1.1%, while oxalate-extractable iron (Fe<sub>o</sub>) ranged from 0.38 to 0.65% with an Fe<sub>o</sub>/(Fe<sub>d</sub>–Fe<sub>o</sub>) ratio of 0.78–2.26. This indicates that Fe oxidation–reduction reactions probably take place in the sediments, given that the proportion of amorphous or poorly crystalline constituents exceeds that of the crystalline forms. Total Mn concentrations ranged from 0.053 to 0.078% in different layers. The mean Mn<sub>d</sub> content was 0.034% while Mn<sub>o</sub> ranged from 0.039 to 0.045%, accounting for 80% of Mn<sub>d</sub> content in the sediments.

It appears that the active redox behavior for Fe and Mn influences P migration from the bottom to the top layers, which can be verified by decreases in BD-P or NaOH-P proportions (Fig. 2) with increasing depth, as their abundance. The specific mechanisms of P transport and transformation in this studied area have been discussed by Xie et al. [19] in details.

### 3.2. Effect of ion solutions on P adsorption

Under natural conditions, the P concentration of the ambient solution (overlying water or pore water) is generally not as high as the several to tens of mg per L as reported in many studies [26,27], in which data-sets usually fit well with Langmuir or Freundlich isotherm models under high P concentrations. The data-sets obtained in our research fit well with the

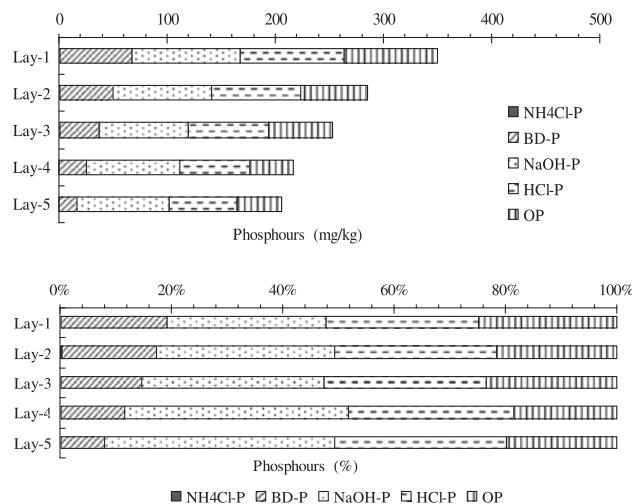


Fig. 2. Profiles of P composition in the sediment cores along vertical profiles.

linear model of isothermal adsorption. The adsorption equation, characterized parameters ( $k$ ,  $EPC_0$ , and  $b$ ), and statistical features ( $r^2$  for correlation coefficient and  $p$  for judging significant correlation) within different groups of ion solutions are summarized in Tables 5–9, while the isotherm curves ( $Q$  vs.  $C_e$ ) are shown in Figs. 3–7. For ease of comparing and characterizing criteria between different groups and different layers, all figures have been plotted on the same scale.

As shown in Table 5 and Fig. 3, for the group of distilled water solutions, there was an obvious difference of the distribution of P adsorption isotherms between data-sets obtained from the surface and middle-bottom layers. Most isotherms are highly linear. The data-sets for the surface layers were concentrated in the lower left corner of the plot. However, for the middle-bottom layers, the data-sets were concentrated in the upper right corner with better correlations.

Mean  $k$  values (slopes) in the three layers were 118.8, 84.8, and 109.1 L/kg, respectively. They were at rather low ranges and did not show significant differences (comparing means between different layers), indicating relatively weak sorption abilities in this group. Mean  $EPC_0$  values of different sampling sites were 0.32, 0.08, and 0.07 mg/L for the three layers, from the surface to the bottom, respectively, exhibiting significant differences between the surface and middle-bottom layers ( $p < 0.01$ ). For  $b$  values, representing NAP in the sediments, their surface values were bigger than for the other two layers. Obviously, the difference between the middle and bottom layers was not significant since both of them originated from the same submerged soil. The surface sediments presented higher P-releasing potential than the other

Table 5  
Parameters for P adsorption isotherms within the pure water group in sediments from different sites

Layer	No.	$Q = KC_e + b$	$K$	$b$	$R^2$	$p$	$EPC_0$	Mean $EPC_0$
Surface	S1	$y = 68.3826x - 34.363$	68.3826	-34.363	0.458	0.140	0.50	0.32
	S3	$y = 139.897x - 47.849$	139.897	-47.849	0.512	0.110	0.34	
	S5	$y = 122.809x - 33.957$	122.809	-33.957	0.797	0.003**	0.28	
	S7	$y = 125.489x - 28.742$	125.489	-28.742	0.824	0.012*	0.23	
	S9	$y = 137.514x - 36.463$	137.514	-36.463	0.697	0.010**	0.27	
Middle	S1	$y = 79.8881x - 4.4950$	79.8881	-4.4950	0.644	0.017*	0.06	0.08
	S3	$y = 78.2862x - 6.0808$	78.2862	-6.0808	0.920	0.000**	0.08	
	S5	$y = 63.2052x - 7.8795$	63.2052	-7.8795	0.792	0.003**	0.12	
	S7	$y = 97.9403x - 2.0988$	97.9403	-2.0988	0.930	0.000**	0.02	
	S9	$y = 104.565x - 12.141$	104.565	-12.141	0.904	0.000**	0.12	
Bottom	S1	$y = 122.51x - 4.4016$	122.51	-4.4016	0.9378	0.000**	0.04	0.07
	S3	$y = 65.4896x - 3.4812$	65.4896	-3.4812	0.925	0.001**	0.05	
	S5	$y = 43.2064x - 9.7054$	43.2064	-9.7054	0.642	0.05*	0.22	
	S7	$y = 209.459x - 6.7160$	209.459	-6.7160	0.646	0.054	0.03	
	S9	$y = 105.018x - 4.6761$	105.018	-4.6761	0.961	0.000**	0.04	

Note: \* indicates significance correlation at a level of 95% while \*\* for a level of 99%.

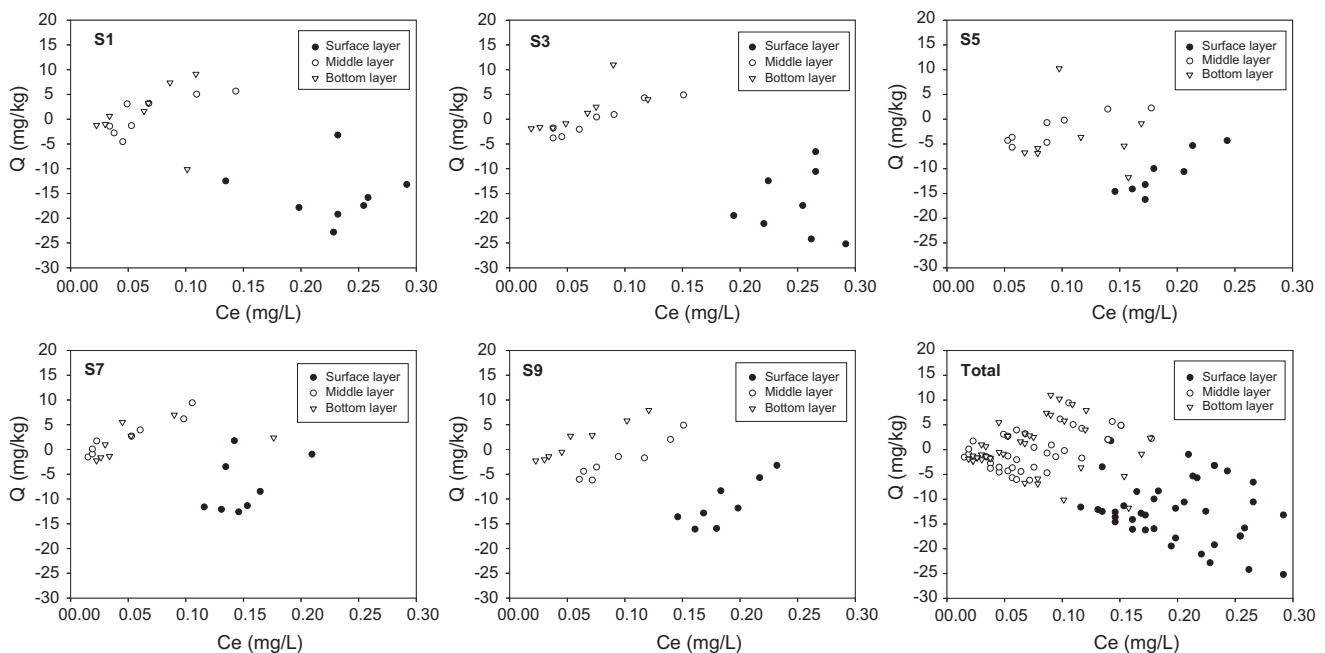


Fig. 3. P adsorption isotherms for the pure water group in the sediments from different sites.

two layers, which was indicated by the characterized parameters of  $EPC_0$  and  $b$  as well.

For adsorption experiments in the NaCl solution group, the linear correlation was greatly higher (see  $p$  values in Table 6). Significant differences in data-sets

between the surface layer and the middle-bottom layers exist, but these were smaller than those observed in the distilled water group (Fig. 4). Mean  $k$  values within these three groups were 168.2, 165.2, and 270.3 L/kg, respectively. No significant difference

Table 6  
Parameters for P adsorption isotherms within the NaCl solution group in the sediments from different sites

Layer	No.	$Q = KC_e + b$	$K$	$b$	$R^2$	$p$	$EPC_0$	Mean $EPC_0$
Surface	S1	$y = 75.8924x - 15.065$	75.8924	-15.065	0.797	0.003**	0.20	0.16
	S3	$y = 268.082x - 36.821$	268.082	-36.821	0.987	0.000**	0.14	
	S5	$y = 171.997x - 24.743$	171.997	-24.743	0.843	0.001**	0.14	
	S7	$y = 185.429x - 20.775$	185.429	-20.775	0.836	0.001**	0.11	
	S9	$y = 13.9569x - 3.0015$	139.569	-3.0015	0.012	0.070	0.22	
Middle	S1	$y = 137.047x - 6.5978$	137.047	-6.5978	0.525	0.042*	0.05	0.08
	S3	$y = 84.688x - 2.7087$	84.688	-2.7087	0.539	0.059	0.03	
	S5	$y = 226.968x - 13.832$	226.968	-13.832	0.860	0.001**	0.06	
	S7	$y = 254.022x - 10.120$	254.022	-10.120	0.838	0.001**	0.04	
	S9	$y = 123.325x - 17.192$	123.325	-17.192	0.838	0.001**	0.14	
Bottom	S1	$y = 416.495x - 16.327$	416.495	-16.327	0.811	0.002**	0.04	0.06
	S3	$y = 164.243x - 10.079$	164.243	-10.079	0.978	0.000**	0.06	
	S5	$y = 120.099x - 11.304$	120.099	-11.304	0.951	0.000**	0.09	
	S7	$y = 438.095x - 20.961$	438.095	-20.961	0.787	0.003**	0.05	
	S9	$y = 212.771x - 12.040$	212.771	-12.040	0.872	0.001**	0.06	

Note: \*indicates significance correlation at a level of 95% while \*\* for a level of 99%.

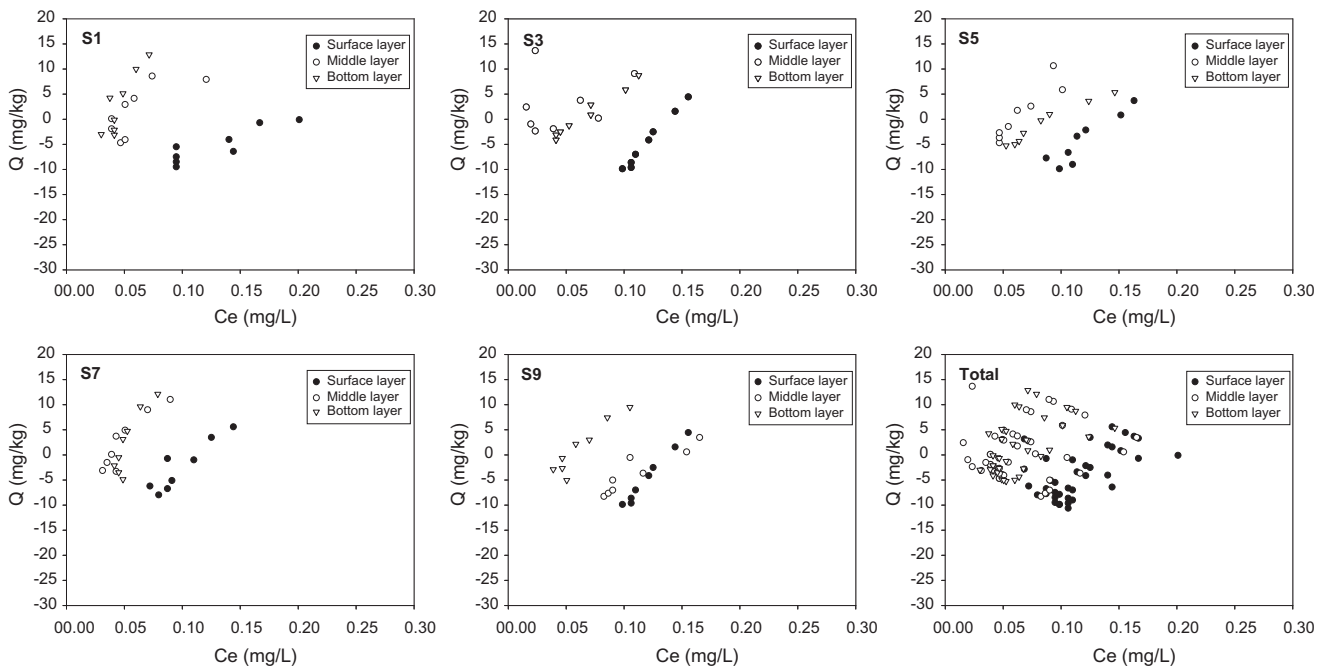


Fig. 4. P adsorption isotherms for the NaCl solution group in the sediments from different sites.

exists between  $k$  values of three layers, though they were slightly higher in the distilled water group than in other groups, and showed an improved ability to “buffer” dissolved phosphorus. Mean  $EPC_0$  values in different sampling sites were 0.16, 0.08, and 0.06 mg/L for the three layers, respectively (Table 6).

Nevertheless, the adsorption potential of P on the surface sediments was still weaker than that for the other two layers.

Regarding isotherms in the  $CaCl_2$  solution group, much smaller differences were observed between the data-sets of the three layers. All data-sets were

clustered in the upper right zone (Fig. 5).  $k$  values were larger compared with those in the groups of distilled water and NaCl solutions, with their mean values of 342.7, 652.3, and 807.5 L/kg, respectively. It suggested the sediment's ability to "buffer" dissolved P by sorbing most of the added P, with steeper isotherms signifying a higher buffering ability. Averaged  $EPC_0$  values were 0.05, 0.02, and 0.02 mg/L for the three layers (Table 7), respectively. All of them were significantly lower than those in the above two groups. It is without doubt that the P adsorption abilities of the sediments were enhanced by the addition of  $CaCl_2$ .

Solutions of  $NaHCO_3$  are weakly alkaline, distinguishing them from other treated samples within this study. Most data-sets appeared to cluster or even to overlap in some sites (Fig. 6). The  $k$  values suggested smaller slopes compared with those in the above three groups, with mean values of 65.1, 53.6, and 51.2 L/kg, indicating their weaker "buffering capacity" for increasing P concentration. Averaged  $EPC_0$  values were 0.19, 0.17, and 0.12 mg/L for the three layers, respectively (Table 8). Apparently, an alkaline environment can significantly decrease the ability for P to adsorb on to surface sediments, regardless of which layer the sediments originated from.

The  $NaHCO_3 + CaCl_2$  solution group approximates the water chemistry in the researched area. Based on the data-sets and their cluster distribution, it can be

observed that this group is intermediate between the  $CaCl_2$  and  $NaHCO_3$  solution groups, namely, closer to the upper right zone in  $CaCl_2$  solutions but smaller slopes of these curves (Fig. 7). Mean  $k$  values were 186.2, 385.6, and 363.0 L/kg for the three layers, respectively. Their  $EPC_0$  values were still small with values of 0.06, 0.04, and 0.02 mg/L (Table 9), indicating that  $CaCl_2$  has a more dominant effect than  $NaHCO_3$  or other weakly alkaline salts.

In order to observe the different solutions' individual effects on P adsorption, the figures were redrawn to assist in an overall comparison between the effects of different solutions on the sediments of the surface and bottom layers (Fig. 8). For surface sediments, data-sets were classified into three zones, whereby the group with distilled water exhibited the weakest P adsorption, followed by the zones with solutions containing NaCl or  $NaHCO_3$ , and finally by the zones containing  $CaCl_2$  or  $NaHCO_3 + CaCl_2$ . The last zone witnessed the best effects in terms of increasing P adsorption.

For the middle-bottom sediments (Fig. 9 only indicates data from the bottom layers), which originated from submerged soil, the effect is slightly different, with the sequence  $CaCl_2 > NaHCO_3 + CaCl_2 > NaCl > pure\ water > NaHCO_3$ .

We evaluated the relationship between the adsorption parameters and the selected soil properties to obtain further information about the main soil proper-

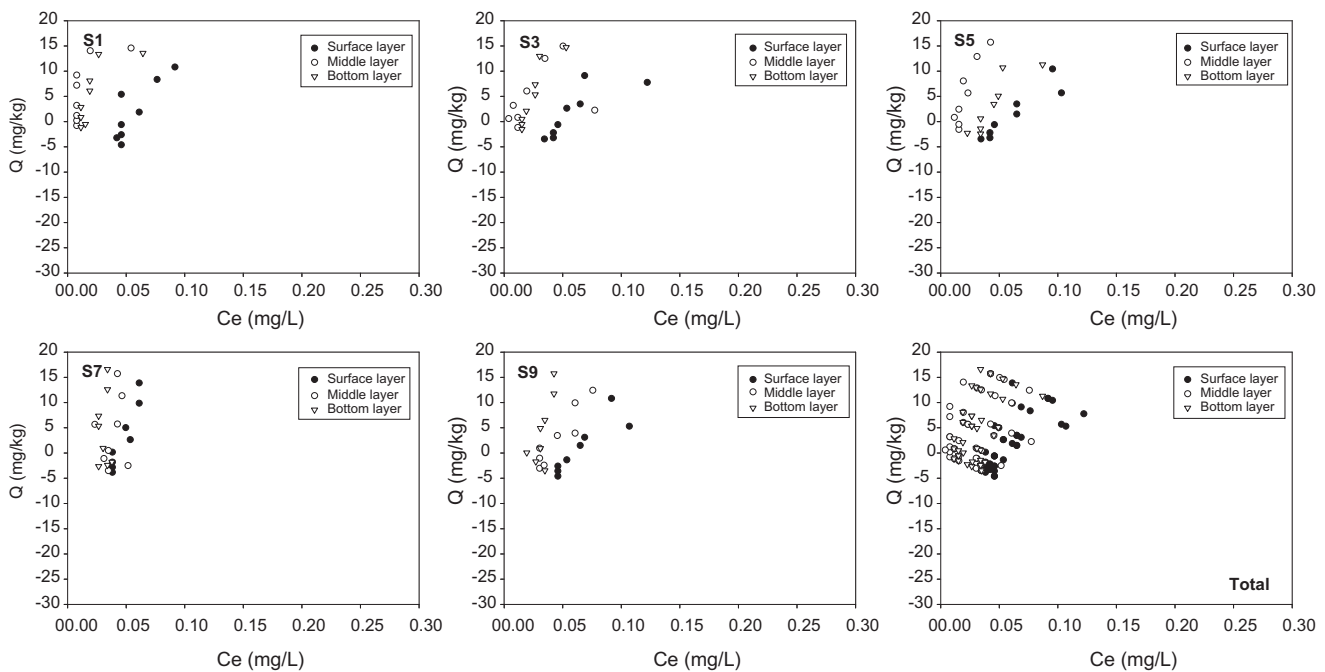


Fig. 5. P adsorption isotherms for the  $CaCl_2$  solution group in the sediments from different sites.

Table 7  
Parameters for P adsorption isotherms within the CaCl<sub>2</sub> solution group in the sediments from different sites

Layer	No.	$Y=QC_e+b$	$K$	$b$	$R^2$	$p$	$EPC_0$	Mean $EPC_0$
Surface	S1	$y=268.962x-13.360$	268.962	-13.360	0.732	0.007**	0.05	0.05
	S3	$y=334.377x-15.924$	334.377	-15.924	0.894	0.001**	0.05	
	S5	$y=230.843x-11.957$	230.843	-11.957	0.967	0.000**	0.05	
	S7	$y=572.088x-24.047$	572.088	-24.047	0.886	0.000**	0.04	
	S9	$y=307.362x-17.389$	307.362	-17.389	0.984	0.000**	0.06	
Middle	S1	$y=975.758x-4.4394$	975.758	-4.4394	0.550	0.056	0.00	0.02
	S3	$y=354.655x-1.8074$	354.655	-1.8074	0.883	0.002**	0.01	
	S5	$y=555.742x-6.5496$	555.742	-6.5496	0.852	0.001**	0.01	
	S7	$y=1080.02x-37.157$	1080.02	-37.157	0.723	0.032*	0.03	
	S9	$y=295.156x-10.404$	295.156	-10.404	0.858	0.001**	0.04	
Bottom	S1	$y=843.299x-9.2356$	843.299	-9.2356	0.830	0.004**	0.01	0.02
	S3	$y=780.588x-12.509$	780.588	-12.509	0.922	0.001**	0.02	
	S5	$y=417.214x-14.241$	417.214	-14.241	0.831	0.004**	0.03	
	S7	$y=1331.03x-32.310$	1331.03	-32.310	0.539	0.096	0.02	
	S9	$y=665.464x-16.327$	665.464	-16.327	0.798	0.007**	0.02	

Note: \* indicates significance correlation at a level of 95% while \*\* for a level of 99%.

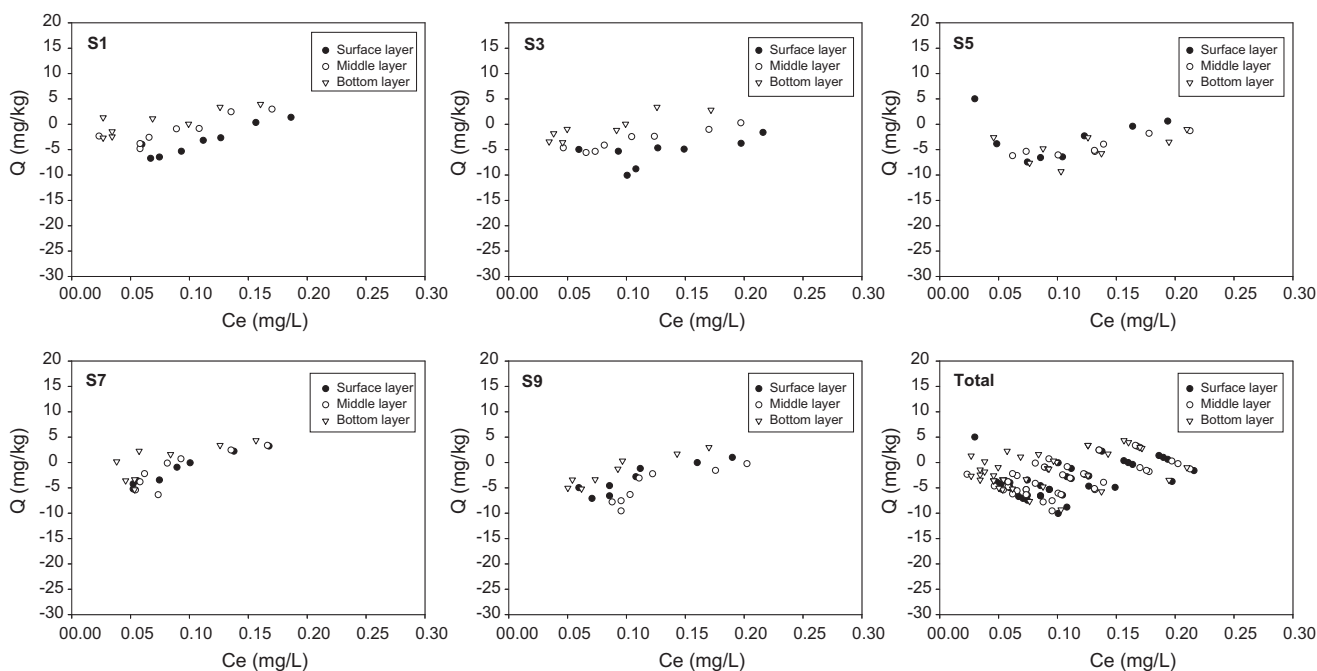


Fig. 6. P adsorption isotherms for the NaHCO<sub>3</sub> solution group in the sediments from different sites.

ties responsible for determining P adsorption as well as P fractionation characteristics. The correlation analysis for different parameters is summarized in Table 10 with BD-P, NaOH-P, and HCl-P as well. Here, we placed emphasis only on P isotherm parameters and selected sediment properties. In most cases,  $EPC_0$

presented significant correlations with BD-P, HCl-P, IP, HCl-P, TP, and OM, but not with OP. However, caution needs to be applied when interpreting the individual effects of these sediment properties on P adsorption due to their significant correlations among one another [27,28]. Considering OM and P-specific

Table 8  
Parameters for P adsorption isotherms within the  $\text{NaHCO}_3$  solution group in the sediments from different sites

Layer	No.	$y = KQC_e + b$	$K$	$b$	$R^2$	$p$	$\text{EPC}_0$	Mean $\text{EPC}_0$
Surface	S1	$y = 61.2458x - 10.011$	61.2458	-10.011	0.857	0.001**	0.16	0.19
	S3	$y = 60.9924x - 14.762$	60.9924	-14.762	0.815	0.014*	0.24	
	S5	$y = 72.0020x - 12.690$	72.0020	-12.690	0.926	0.002**	0.18	
	S7	$y = 70.6388x - 7.9458$	70.6388	-7.9458	0.952	0.000**	0.11	
	S9	$y = 60.8096x - 9.9233$	60.8096	-9.9233	0.814	0.002**	0.16	
Middle	S1	$y = 51.4420x - 5.7587$	51.4420	-5.7587	0.770	0.004**	0.11	0.17
	S3	$y = 37.9167x - 7.2183$	37.9167	-7.2183	0.901	0.000**	0.19	
	S5	$y = 33.7685x - 8.7306$	33.7685	-8.7306	0.818	0.002**	0.26	
	S7	$y = 76.3416x - 8.2898$	76.3416	-8.2898	0.725	0.007**	0.11	
	S9	$y = 68.8207x - 13.309$	68.8207	-13.309	0.718	0.008**	0.19	
Bottom	S1	$y = 40.4887x - 2.4902$	40.4887	-2.4902	0.683	0.011*	0.06	0.12
	S3	$y = 46.8586x - 4.4358$	46.8586	-4.4358	0.796	0.003**	0.09	
	S5	$y = 40.5575x - 10.346$	40.5575	-10.346	0.529	0.064	0.26	
	S7	$y = 61.0005x - 4.7318$	61.0005	-4.7318	0.533	0.040*	0.08	
	S9	$y = 67.4510x - 7.9061$	67.4510	-7.9061	0.903	0.000**	0.12	

Note: \* indicates significance correlation at a level of 95% while \*\* for a level of 99%.

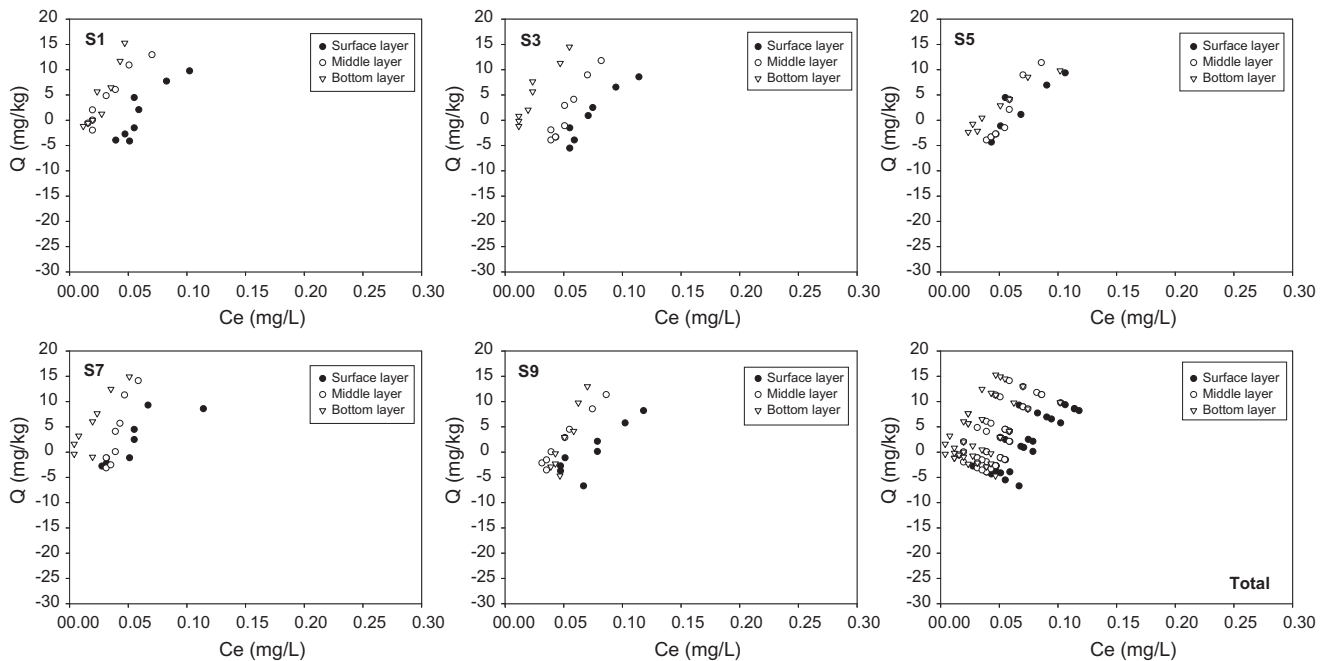


Fig. 7. P adsorption isotherms for the  $\text{NaHCO}_3 + \text{CaCl}_2$  solution group in the sediments from different sites.

fractions as individual variables, it appears that the P desorption potential can be mainly attributed to OM content and inorganic phosphorus. This can also be partly verified by the negative correlation observed between  $k$  values and the inorganic proportion of

P-pools. Therefore, the two characterized parameters in the linear equations describing P adsorption at low P concentrations of aquatic phase,  $k$  and  $\text{EPC}_0$ , can well indicate P release potential and risk.  $k$  indicates the buffer capacity to the added P concentrations

Table 9  
Parameters for P adsorption isotherms within the NaHCO<sub>3</sub>+CaCl<sub>2</sub> solution group in the sediments from different sites

Layer	No.	$y = Kc_e + b$	$K$	$b$	$R^2$	$p$	EPC <sub>0</sub>	Mean EPC <sub>0</sub>
Surface	S1	$y = 234.823x - 12.925$	234.823	-12.925	0.817	0.002**	0.06	0.06
	S3	$y = 204.487x - 13.917$	204.487	-13.917	0.887	0.000**	0.07	
	S5	$y = 199.887x - 11.230$	199.887	-11.230	0.846	0.001**	0.06	
	S7	$y = 129.394x - 5.5327$	129.394	-5.5327	0.850	0.003**	0.04	
	S9	$y = 162.252x - 11.716$	162.252	-11.716	0.736	0.006**	0.07	
Middle	S1	$y = 277.422x - 4.9721$	277.422	-4.9721	0.925	0.000**	0.02	0.04
	S3	$y = 367.947x - 17.761$	367.947	-17.761	0.942	0.000**	0.05	
	S5	$y = 367.103x - 19.117$	367.103	-19.117	0.926	0.000**	0.05	
	S7	$y = 653.300x - 22.884$	653.300	-22.884	0.890	0.000**	0.04	
	S9	$y = 262.148x - 10.754$	262.148	-10.754	0.973	0.000**	0.04	
Bottom	S1	$y = 460.932x - 8.0811$	460.932	-8.0811	0.906	0.000**	0.02	0.02
	S3	$y = 333.368x - 3.5342$	333.368	-3.5342	0.928	0.000**	0.01	
	S5	$y = 166.723x - 5.8112$	166.723	-5.8112	0.939	0.000**	0.03	
	S7	$y = 314.803x - 0.0802$	314.803	-0.0802	0.964	0.000**	0.00	
	S9	$y = 539.241x - 25.456$	539.241	-25.456	0.867	0.001**	0.05	

Note: \*\* indicates significance correlation at a level of 99%.

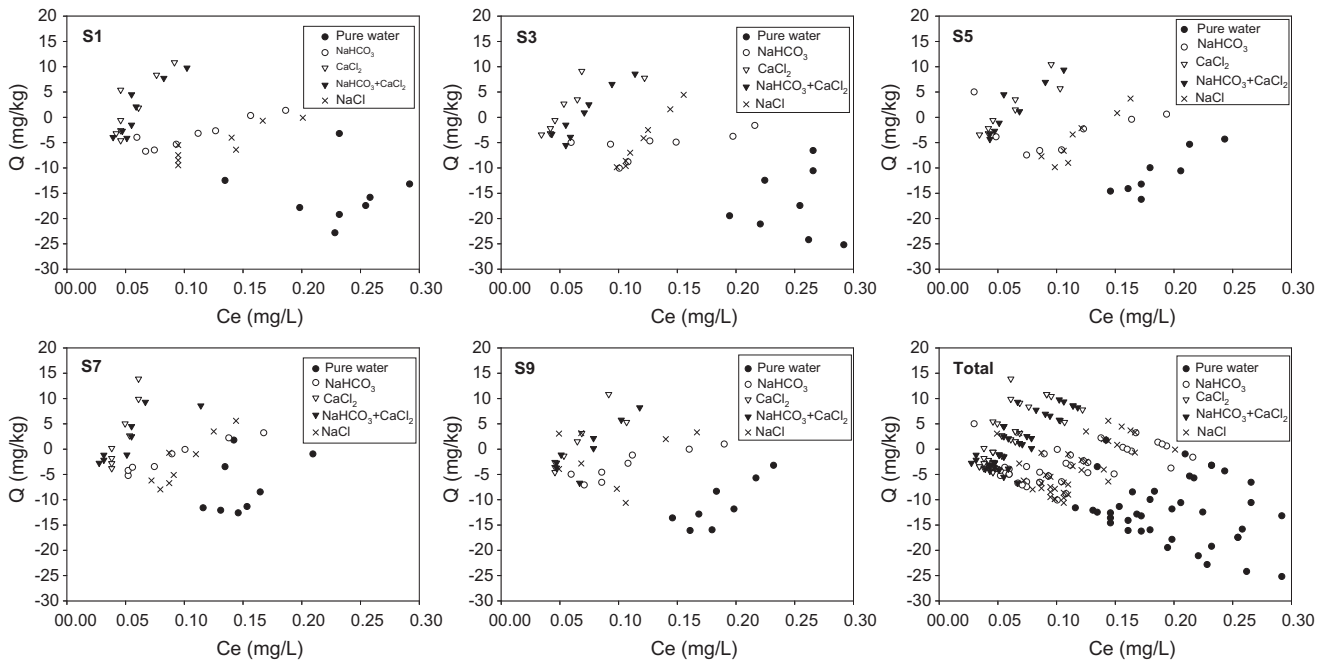


Fig. 8. Comparison of P adsorption isotherms on the surface layer of sediments within different ion solution groups.

while EPC<sub>0</sub> gives the thresholds of P concentration, whether sorbing or desorbing P, by the sediments at a given P solutions.

In resembling previous study which closely resembles this research [29], it was found that EPC<sub>0</sub> and  $k$

have a significantly negative correlation. However, they were usually site-specific based on soil or sediments properties.  $k$  values were determined to have ranges from those smaller than 100 L/kg to greater than 1,000 L/kg, while EPC<sub>0</sub> values were determined

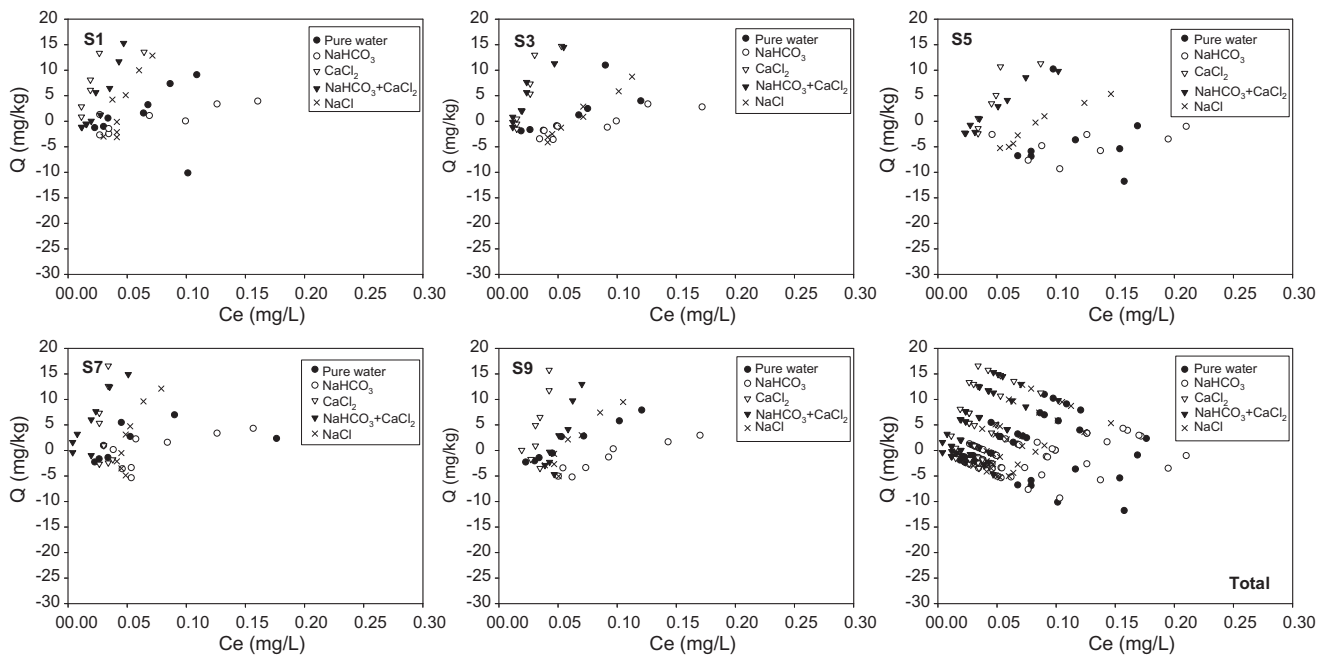


Fig. 9. Comparison of P adsorption isotherms on the bottom layer of sediments in different ion solution groups.

to vary from smaller than  $1\mu\text{g/L}$  to bigger than  $1\text{mg/L}$ . In the five various ion solutions studied in this research, both  $k$  and  $\text{EPC}_0$  showed significant differences, emphasizing the influence of the ambient environment solutions on P adsorption characteristics as well as soils/sediments characteristics.

The local soil texture is a clay loam with a clay content of 20–40% according to the analysis of its particle size distributions. Soils or sediments are a complex of OM and clay soil particles; their proportions and the structure of this complex are important in determining the transport of P and other micronutrients [30]. Clay particles have a larger total surface area while OM indicates that more active sites are available for anions to interact. During lake sedimentary processes, the OM content and active site number in the sediments are probably higher than those in inundated soils. Naturally, the adsorbed P can be easily desorbed to the ambient solution, resulting in higher observed values of  $\text{EPC}_0$  in the surface sediments. This is particularly the case under weak alkaline conditions, where the solid phase tends to be negatively charged, and where  $\text{OH}^-$  competes with phosphate anions at active adsorption sites and causes P adsorption potential to be decreased.

In studies involving lake sediments or wetland soils, the ratio of Fe: P [31] or  $\text{FeO}_x$ : Fe-P is usually used to estimate the P-releasing risk [8]. The total iron content in the studied area was determined to be

rather high, with a Fe: P ratio as high as 122–155. Moreover, the  $\text{FeO}_x$ : Fe-P ranged from 68 to 164 in the sediments of different layers. Both of them greatly exceeded the ratio of 15 of total Fe to P, which was recommended in the literature [31] for indicating less P-releasing risk below this value. Therefore, it can be concluded that the presence of abundant iron oxides, determined by local geological conditions, indicates stronger P adsorption potentials ( $\text{EPC}_0$  values were observed to be as low as  $0.02\mu\text{g/L}$ ). This also can be verified by the P-fraction features, where the sum of BD-P and NaOH-P exceeded HCl-P.

Under the actual conditions of the local water chemistry, the positive effects of  $\text{Ca}^{2+}$  ions on P adsorption prevailed over the negative effects of weakly alkaline conditions. The CEC of the sediments was estimated to be around  $20\text{cmol/kg}$ , supplying enough cationic ions for exchange or pH buffer capacity with the ambient solution. If there is water exchange between the shallow ground water and surface water,  $\text{Ca}^{2+}$  ion movement between the interfaces probably enhances phosphate adsorption through co-precipitation or partition of phosphates on calcite surfaces.

#### 4. Conclusions

The P adsorption behavior in the sediments of the studied water bodies, which originated from

Table 10  
Pearson correlation coefficients of sediment properties and P adsorption parameters

	NH <sub>4</sub> Cl -P	BD -P	NaOH -P	HCl -P	IP	OP	TP	Fe <sub>o</sub>	OM	Clay	CEC	K	EPC <sub>0</sub>
NH <sub>4</sub> Cl-P	1.000												
BD-P	0.556*	1.000											
NaOH-P	0.085	0.207	1.000										
HCl-P	0.205	0.477	-0.406	1.000									
IP	0.316	0.730**	0.514*	0.533*	1.000								
OP	0.346	0.497	-0.250	0.283	0.004	1.000							
TP	0.434	0.871**	0.356	0.602*	0.903**	0.434	1.000						
Fe <sub>o</sub>	0.092	0.027	0.862**	-0.212	0.225	-0.350	0.052	1.000					
OM	0.311	0.676**	-0.212	0.743**	0.527*	0.615*	0.739**	-0.441	1.000				
Clay	-0.111	-0.346	0.317	-0.846*	-0.515*	-0.006	-0.466	0.420	-0.410	1.000			
CEC	0.226	0.003	0.305	-0.600*	-0.248	0.317	-0.087	0.289	-0.056	0.713**	1.000		
K	-0.168	0.066	-0.433	0.140	-0.148	0.211	-0.043	-0.353	0.446	0.064	0.134	1.000	
H <sub>2</sub> O	-0.627*	-0.567*	-0.048	-0.492	-0.476	-0.199	-0.515*	0.072	-0.268	0.453	0.129	1.000	
NaCl	-0.194	-0.611*	-0.268	-0.607*	-0.796**	-0.114	-0.767**	0.080	-0.424	0.563*	0.346	1.000	
CaCl <sub>2</sub>	0.158	0.417	-0.386	0.521*	0.115	0.651**	0.384	-0.356	0.713**	-0.264	-0.011	1.000	
NaHCO <sub>3</sub>	-0.096	-0.487	-0.252	-0.279	-0.504	-0.093	-0.494	-0.124	-0.444	0.046	0.153	1.000	
NaHCO <sub>3</sub> + CaCl <sub>2</sub>	0.214	0.664**	0.391	0.352	0.669**	0.448	0.795**	0.167	0.505	-0.251	0.015	-0.082	1.000
H <sub>2</sub> O	0.510	0.740**	0.128	0.602*	0.689**	0.531*	0.849**	-0.066	0.758**	-0.390	-0.201	-0.535*	1.000
NaCl	0.278	0.621*	-0.040	0.728**	0.640*	0.503	0.793**	-0.255	0.853**	-0.508	-0.161	-0.596*	1.000
CaCl <sub>2</sub>	0.001	0.331	0.430	0.398	0.699**	-0.223	0.534*	0.174	0.105	-0.433	-0.013	-0.267	1.000
NaHCO <sub>3</sub>	0.334	0.767**	0.156	0.635*	0.774**	0.383	0.862**	-0.201	0.577**	-0.617*	-0.193	-0.221	1.000

Note: \*  $p < 0.05$ ; \*\*  $p < 0.01$ ;  $n = 23$ .

subsidence and submergence of agricultural land by coal mine activities in the Huaibei Plain Area, was well documented in this study, with special considerations given to the local water chemistry. The key conclusions can be summarized as follows:

(1) In water bodies with relatively long histories spanning several decades, significant quantities of sedimentary matter accumulated on the submerged soil layers, ultimately leading to differentiation of the sediments' properties and adsorption features, such as OM and TP and its fractions,  $EPC_0$ ,  $k$  values, etc.

(2) Ion solution effects on P adsorption are important. Usually,  $Ca^{2+}$  can enhance P adsorption on sediment surfaces, while weakly alkaline conditions caused by bicarbonates are unfavorable for its adsorption. As a comprehensive effect, the positive effect of the former is greater than the negative effect of the latter, probably due to cationic exchange or buffer capacities supplied by the sediment surface.

(3) The presence of abundant Fe oxides and dynamic redox conditions could result in low  $EPC_0$  values and a high proportion of TP that is bound to metal oxides. However, further emphasis should be placed on the risk of P release if the sediment surfaces suffer anoxic or anaerobic transformation caused by heavy OM pollution, fish feeding, or external pollutant drainage.

### Acknowledgements

This work was supported by project of the Natural Science Foundation of China (Grant No. 41202242), the Natural Science Research Project of Anhui Provincial University funded by the Anhui Education Department (Grant No. KJ2011A084), and the China Postdoctoral Science Foundation Funded Project (Grant No. 20110490814). Additional support came from the 2010 research project of "Environmental Impact of Coal Mining Activities on the Surface Water and Shallow Groundwater in the Panxie Coal Mine Area," which was funded by the National Engineering Laboratory of Ecological and Environmental Protection of China, Huainan Mining Group Company.

### References

- [1] H.E. Fang, X.U. You-ning, Q.I.A.O. Gang, L.I.U. Rui-p, Regional distribution characteristics of mine environmental geological problems in China, *Geol. China* 5 (2010) 1520–1528.
- [2] A. Kaiserli, D. Voutsas, C. Samara, Phosphorus fractionation in lake sediments-Lakes Volvi and Koronia, N Greece, *Chemosphere* 46 (2002) 1147–1155.
- [3] L.Q. Xie, P. Xie, H.J. Tang, Enhancement of dissolved phosphorus release from sediment to lake water by Microcystis blooms—an enclosure experiment in a hyper-eutrophic, subtropical Chinese lake, *Environ. Pollut.* 122 (2003) 391–399.
- [4] S. Wang, X.C. Jin, H.C. Zhao, F.C. Wu, Phosphorus fractions and its release in the sediments from the shallow lakes in the middle and lower reaches of Yangtze River area in China, *Colloids Surf. A* 273 (2006) 109–116.
- [5] N. Chacon, W.L. Silver, E.A. Dubinsky, D.F. Cusack, Iron reduction and soil phosphorus solubilization in humid Tropical forests soils: The roles of labile carbon pools and an electron shuttle compound, *Biogeochemistry* 78 (2005) 67–84.
- [6] N. Chacon, S. Flores, A. Gonzalez, Implications of iron solubilization on soil phosphorus release in seasonally flooded forests of the lower Orinoco River Venezuela, *Soil Biol. Biochem.* 38 (2006) 1494–1499.
- [7] O.G. Olila, K.R. Reddy, D.L. Stites, Influence of draining on soil phosphorus forms and distribution in a constructed wetland, *Ecol. Eng.* 9 (1997) 157–169.
- [8] R. Loeb, L.P.M. Lamers, J.G.M. Roelofs, Prediction of phosphorus mobilization in inundated floodplain soils, *Environ. Pollut.* 156 (2008) 325–331.
- [9] E.J. Dunnea, M.W. Clark, J. Mitchell, J.W. Jawitz, K.R. Reddy, Soil phosphorus flux from emergent marsh wetlands and surrounding grazed pasture uplands, *Ecol. Eng.* 36 (2010) 1392–1400.
- [10] Hefei Design Research Institute for Coal Industry (HDRICI), Geographical Environment Survey of Panxie Mining Area, HDRICI, Hefei, 1986.
- [11] A.M. Zhou, H.X. Tang, D.S. Wang, Phosphorus adsorption on natural sediments: Modeling and effects of pH and sediment composition, *Water Res.* 39 (2005) 1245–1254.
- [12] S. Tunesi, V. Poggi, C. Gessa, Phosphate adsorption and precipitation in calcareous soils: the role of calcium ions in solution and carbonate minerals, *Nutr. Cycling Agroecosyst.* 53 (1999) 219–227.
- [13] M. Dittrich, O. Gabriel, C. Rutzen, R. Koschel, Lake restoration by hypolimnetic  $Ca(OH)_2$  treatment: Impact on phosphorus sedimentation and release from sediment, *Sci. Total Environ.* 8 (2011) 1504–1505.
- [14] Y. Ann, K.R. Reddy, J.J. Delfino, Influence of redox potential on phosphorus solubility in chemically amended wetland organic soils, *Ecol. Eng.* 14 (2000) 169–180.
- [15] W.A. House, F.H. Zenison, Factors influencing the measurement of equilibrium phosphate concentrations in river sediments, *Water Res.* 34 (2000) 1187–1200.
- [16] L.D. Huang, L.L. Li, L.C. Huang, G. Gielen, Y.S. Zhang, H.L. Wang, Influence of incubation time on phosphorus sorption dynamics in lake sediments, *J. Soils Sediments* 12 (2012) 443–455.
- [17] M.L. Machesky, T.R. Holm, J.A. Slowikowski, Phosphorus speciation in stream bed sediments from an agricultural watershed: Solid-phase associations and sorption behavior, *Aquat. Geochem.* 16 (2010) 639–662.
- [18] APHA, AWWA, and WPCF, Standard Methods for the Examination of Water and Wastewater, sixteenth ed., APHA, AWWA, WPCF, Washington, DC, 1998.
- [19] K. Xie, Y.Q. Zhang, Q.T. Yi, J.P. Yan, Phosphorus fractions and migration in the sediments of a subsided water area in Panyi Coal Mine of Huainan, China *Environ. Sci.* 10 (2012) 1867–1874.
- [20] R.E. Carson, Atrophic state index for lakes, *Limno. Oceanogr.* 2 (1977) 361–369.
- [21] R.K. Lu, Chemical Analysis Methods of Agricultural Soils, China Agricultural Science Press, Beijing, 1999.
- [22] K.H. Tan, Soil Sampling Preparation and Analysis, Marcel Dekker, New York, NY, 1995.
- [23] R. Psenner, Fractionation of phosphorus in suspended matter and sediment, *Ergebnisse Limno* 30 (1988) 98–113.
- [24] M. Hupfer, R. Gachter, R. Giovanoli, Transformation of phosphorus species in settling seston and during early sediment diagenesis, *Aquat. Sci.* 57 (1995) 305–324.
- [25] Q. Zhou, C.E. Gibson, Y. Zhu, Evaluation of phosphorus bioavailability in sediments of three contrasting lakes in China and the UK, *Chemosphere* 42 (2001) 221–225.

- [26] D.S. Ting, A. Appan, General characteristics and fractions of phosphorus in aquatic sediments of two tropical reservoirs, *Water Sci. Technol.* 7–8 (1996) 53–59.
- [27] G.J. Lair, F. Zehetner, Z.H. Khan, M.H. Gerzabek, Phosphorus sorption-desorption in alluvial soils of a young weathering sequence at the Danube River, *Geoderma* 149 (2009) 39–44.
- [28] D.Y.F. Lai, K.C. Lam, Phosphorus sorption by sediments in a subtropical constructed wetland receiving stormwater runoff, *Ecol. Eng.* 35 (2009) 735–743.
- [29] G.J. Kerr, M. Burford, J. Olley, J. Udy, Phosphorus sorption in soils and sediments: implications for phosphate supply to a subtropical river in southeast Queensland Australia, *Biogeochemistry* 102 (2011) 73–85.
- [30] J.G. Cai, *Organic Clay Complex of the Mud Sediments and Argillaceous Rocks*, Science Press of China, Beijing, 2004.
- [31] H.S. Jensen, P. Kristensen, E. Jeppesen, A. Skytthe, Iron phosphorus ratio in surface sediment as an indicator of phosphate release from aerobic sediments in shallow lakes, *Hydrobiologia* 235 (1992) 731–743.